Tracking Performance of the Transition Radiation Tracker Prototype for the ATLAS Experiment

T. Akesson [a], K. Baker [b], V. Bondarenko [c], V. Bytchkov [d], H. Carling [a], H. Danielsson [a,e], F. Dittus [f], B. Dolgoshein [c], N. Dressnandt [g], W. L. Ebenstein [h], P. Eerola [a], U. Egede [a], P. Farthouat [f], D. Froidevaux [f], I. Gavrilenko [i], Y. Grichkevitch [j], Z. Hajduk [k], G. Hanson [l], V.G. Ivochkin [m], S. Jagielski [n], P.T. Keener [g], S. Konovalov [i], G. Kekelidze [d], V.A. Kramarenko [j], A. Laritchev [j], P. Lichard [f], B. Lundberg [a], F. Luehring [l], K. McFarlane [b], S. Muraviev [i], A. Nadtochy [m], P. Nevski [c,o], F.M. Newcomer [g], H. Ogren [l], S.H. Oh [h], V. Peshekhonov [d], A. Romaniouk [c,e], D.R. Rust [l], V. Schegelsky [m], S. Semenov [c], A. Shmeleva [i], S. Smirnov [c], L.N. Smirnova [j], V. Sosnovtsev [c], E. Spiridenkov [m], M. Stavrianakou [f], M. Thulesius [a], V. Tikhomirov [i], R. Van Berg [g], C. Wang [h], H.H. Williams [g]

[a] *Fysiska Institutionen, Lunds Universitet, Lund, Sweden*

[b] *Hampton University, Hampton, Virginia, USA*

[c] *Moscow Engineering and Physics Institute, Moscow, Russia*

[d] *Joint Institute of Nuclear Research, Dubna, Russia*

[e] *now at CERN, Geneva, Switzerland*

[f] *European Laboratory for Particle Physics (CERN), Geneva, Switzerland*

[g] *Department of Physics and Astronomy, University of Pennsylvania, Philadelphia, Pennsylvania, USA*

[h] *Physics Department, Duke University, Durham, North Carolina, USA*

[i] *P.N. Lebedev Institute of Physics, Moscow, Russia*

[j] *Moscow State University, Institute of Nuclear Physics, Moscow, Russia*

[k] *Henryk Niewodniczanski Institute of Nuclear Physics, Cracow, Poland*

[l] *Indiana University, Bloomington, Indiana, USA*

[m] *Petersburg Nuclear Physics Institute, Gatchina, St. Petersburg, Russia*

[n] *Faculty of Physics and Nuclear Techniques of the Academy of Mining and Metallurgy, Cracow, Poland*

Preprint submitted to Elsevier Preprint *16 March 2001*

°*now at Brookhaven National Laboratory, New York, USA*

ATLAS TRT collaboration

Abstract

A prototype of the Transition Radiation Tracker (TRT) for the ATLAS experiment at the CERN LHC has been built and tested at the CERN SPS. Detailed studies of the drift-time measurements, alignment technique, hit registration efficiency, track and momentum accuracy were performed. A coordinate measurement accuracy of 150 μm for a single TRT drift tube and momentum resolution of 0.8% for 20 GeV pions in a 1.56 T magnetic field were achieved. The results obtained are in agreement with the expected tracking performance of the ATLAS TRT.

Key words: ATLAS. Transition radiation. Drift-time measurement. Tracking. Coordinate accuracy. Hit registration efficiency. Momentum resolution.

1 Introduction

The ATLAS Transition Radiation Tracker (TRT) [1] combines electron identification capability with charged particle track reconstruction. This feature is achieved by interleaving layers of xenon-filled drift tubes of small diameter (straws) with radiator. The signals from transition radiation (TR) photons are thus recorded in the same detecting elements as those used to reconstruct the track, in contrast to the methods, in which the particle trajectory is measured in one device and an extrapolation is needed to look for the signal from transition radiation photons in a dedicated detector. This combination of tracking and transition radiation detection in the ATLAS TRT strengthens the particle identification power, since the measurements of the transition radiation photons can be assigned correctly to the reconstructed track. The TRT provides many measurement points on a charged particle trajectory, ensuring robust pattern recognition at the high track multiplicities expected at the LHC design luminosity.

To test the physics performance of the proposed detector, a small-scale TRT prototype with a geometry close to that of the ATLAS end-cap TRT was built and tested. Results on particle identification with this TRT prototype have been reported in Ref. [2]. This paper presents the results of tracking studies using the drift-time information from the straws. The experimental setup is described in section 2. Section 3 presents a Monte Carlo model developed to reproduce our experimental observations. A detailed description of drift-time measurement techniques is presented in section 4. In section 5 the geometrical alignment procedure is described. Hit registration efficiency is discussed in section 6. Tracking performance without and with magnetic field is reported in sections 7 and 8 respectively. Summary and conclusions are collected in section 9.

2 Experimental setup

The TRT prototype was tested in the H8 beam line at the CERN SPS during several periods in 1995 and 1996. The TRT performance was evaluated using electron and pion beams with energies from 20 to 200 GeV. The layout of the test-beam setup is shown in Figure 1. Three precise silicon microstrip detectors and two gaseous beam chambers formed a beam telescope. A Cherenkov counter (not shown here) and a preshower detector together with a small lead-glass electromagnetic calorimeter were used for beam pion/electron separation. The total amount of material in front of the TRT detector was about 11% of a radiation length.

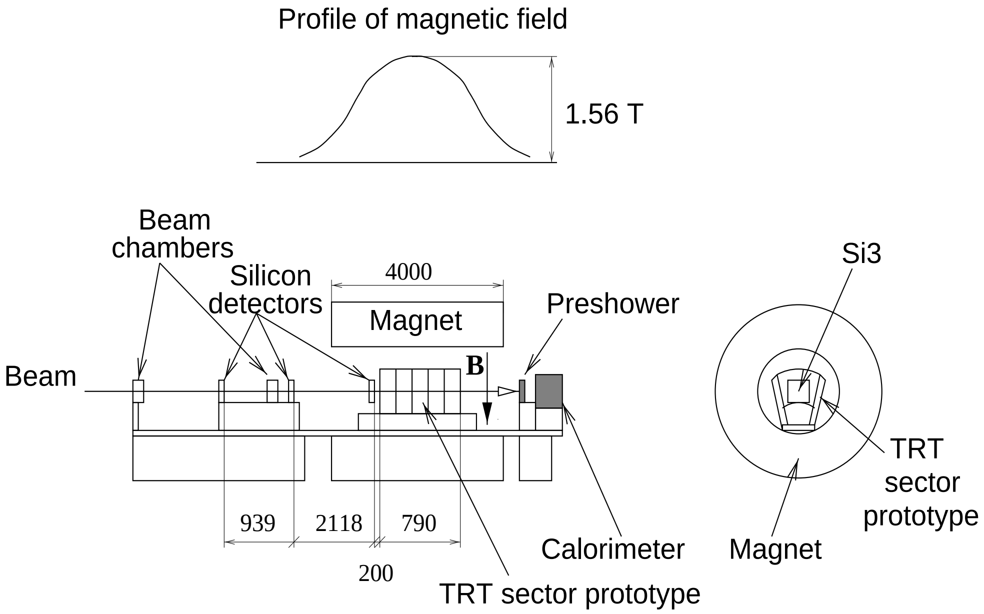

Fig. 1. TRT sector prototype setup in test-beam run. Side view (left) and downstream view (right). All distances are in mm. The drawing is not to scale.

The TRT prototype represented a 30 degree sector of the ATLAS end-cap TRT and was equipped with LHC-type electronics. The prototype consisted of five blocks containing 512 straw drift tubes each. Each block (Figure 2) contained 16 layers of radially distributed straws. The space between the layers (9.75 mm) was filled with radiator (17 polypropylene foils of 15 μm thickness, spaced by 265 μm). Layers were staggered with respect to each other to minimise the fluctuations in the number of straws crossed by beam particles at different impact points on the prototype. The straw tubes (4 mm in diameter and 33 cm long) were made from conductive Kapton film of 60 μm thickness and were reinforced by carbon fibres glued to the outer surface of the straw. The anode wire, made from gold-plated tungsten, had a diameter of 50 μm.

The straws were operated with a gas mixture consisting of 70% Xe, 20% CF_4 and 10% CO_2. This mixture combines the advantages of efficient TR-absorption, short drift time and good stability. The gas flow was 0.05 cm^3/min per straw, which corresponds to about one volume per hour. The gas gain was $2.5{\cdot}10^4$ and was monitored using a Fe^{55} source.

The electronics used for this prototype test was designed to fulfil all the basic requirements needed to ensure operation in the LHC environment, including the 40 MHz bunch crossing rate. The Transition Radiation Detector Analogue (TRDA) integrated circuit [3,4] included a preamplifier, a shaper and two discriminators with adjustable thresholds. A low-level threshold (typically set to 200 eV) was used to detect the signal from minimum-ionising particles. The resulting signal was used for drift-time measurements. A high-level threshold was set typically to 6 keV to register the absorbed transition radiation pho-

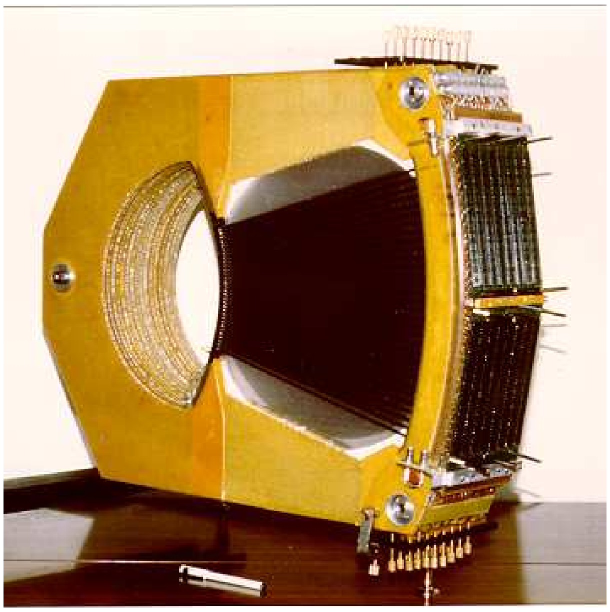

Fig. 2. One of the five blocks of the TRT prototype. Each block contains 512 radial straws. The front-end electronics are connected to the outer periphery of the module.

tons, which produce large signals. The Transition Radiation Detector Service (TRDS) chip [5] received the signals from the TRDA chip, decoded and converted them into standard CMOS signals. The drift time was measured by the 32-channel Drift-Time Measuring Readout Chip (DTMROC) [6] with 3.125 ns binning.

The front-end electronics, assembled on one board, was placed directly on the detector. It was connected to the supervisor module (Local Logic), which collected all the data, packed and sent them to the Data Acquisition system. The maximum collection time (drift time) of ionisation electrons in the straw gas was about 40 ns. The output analogue signal had a peaking time of 12.5 ns and a fall time of about 15 ns. Special attention was paid to accurate cancellation of the long ion tail observed in the straw signal to avoid baseline shifts at high counting rates.

The total length of the TRT prototype along the beam direction was 780 mm. The average thickness of the prototype was 12% of a radiation length for particles at normal incidence. The prototype was placed inside a superconducting magnet with a maximum magnetic field of 1.56 T. The straw orientation was perpendicular to the beam and almost parallel to the magnetic field, corresponding to the layout foreseen in the ATLAS TRT at central rapidities.

A detailed description of the TRT Sector Prototype, straw properties and TRT electronics can be found in Refs. [1], [2], [7] and [8].

3 Monte Carlo simulation

A Monte Carlo model was developed to describe the TRT prototype tracking performance. This program was based on GEANT3 [9], the ATLSIM [10] package, and a sector prototype geometry description program [11]. It simulated in detail the silicon telescope and the TRT prototype. The other parts of the beam line were included only as passive material.

The simulation of the TRT included:

- A detailed simulation of the charged particle energy loss in the straw gas according to the Photo-Absorption Ionisation (PAI) model [12].
- Production and absorption of transition radiation photons. This part was simulated by a special subprogram, because GEANT3 does not contain transition radiation as a physical process.
- Response of the straws to the energy deposited by ionising particles or photons. The drift of ionisation clusters to the anode in the straw gas was included.
- Convolution of the straw output signal with a model of the front-end electronics signal shape.
- Response of the low- and high-threshold discriminators.

Some additional tuning of the Monte Carlo model was made to simulate the real TRT prototype properties as closely as possible:

- An efficiency table for each straw electronics channel was derived from the experimental data and applied to the Monte Carlo.
- An initial random misalignment of r.m.s. 58 μm (see Section 5 and Figure 6) was applied to each anode wire position.
- An exact map of the magnetic field was used.

Simulated data were recorded in exactly the same format as the experimental data. Both data sets were processed with the same program. The Monte Carlo results agree well with the data, as shown in the following sections.

4 Drift-time measurement

All results on drift-time measurements, alignment procedure and hit registration efficiency were obtained with a 20 GeV pion beam, since this data set had the largest statistics. To reconstruct the position of the beam particle crossing a straw, it is necessary to establish the dependence of the particle's radial coordinate with respect to the anode wire (R) on the measured drift time (t)

of ionisation electrons and to determine the anode coordinate itself. The latter represents the geometrical alignment procedure and will be discussed in the next section.

The reference position of the beam track in the TRT prototype was found using information from the Si-microstrip telescope. The intrinsic spatial resolution of the Si detectors was about 10 μm, but multiple scattering also affected somewhat the reconstruction accuracy of the beam track. Figure 3 shows the correlation between the measured drift time t in the straw and the distance R between the anode wire and the extrapolated position of the beam track. The radius-to-time relationship for the straw was then obtained by fitting each of the left and the right branches of this two-dimensional plot with a third-degree polynomial of the form:

$$R = a + bt + ct^2 + dt^3 \tag{1}$$

Once the parameters of the above formula are known, the drift-time measurement can be converted into a distance from the straw anode, and residuals with respect to the position of the extrapolated beam track can be extracted. An example is shown in Figure 4. The single straw coordinate measurement accuracy was defined from this distribution as the standard deviation σ of a Gaussian fit within a range of $\pm 2\sigma$ (approximately ± 300 μm here) around the peak position. The non-Gaussian part of the residual distribution arises mainly from tracks crossing the straw near the wire and from long-range δ-electrons knocked out by the beam particle and also from electronics noise and pickup. The contribution to the width of the distribution from the extrapolation of the beam track measurement and from multiple scattering has to be taken into account (see below).

The straw coordinate measurement accuracy as a function of the low-level electronics threshold is shown in Figure 5. Each point represents the result obtained by averaging over several calibrated straws from the first TRT block (see explanation below). At the proposed ATLAS TRT operating threshold of 200 eV, the coordinate measurement accuracy is around 150 μm and degrades to about 170 μm for higher threshold of 400 eV. In the following, all results were obtained with the nominal 200 eV threshold, unless stated otherwise.

It was found that the straw spatial resolution is around 150 μm for the straws in the first TRT block but is worse for the other blocks, due (in part) to the increasing beam track extrapolation error, and mostly to multiple scattering of the 20 GeV beam particles inside the TRT. The Monte Carlo simulations take these effects into account and describe well the dependence of the straw coordinate measurement accuracy as a function of the depth of the straw inside the TRT prototype. The accuracy typically degrades from about 150 μm for the first block to about 190 μm for the last block in the case of the 20 GeV

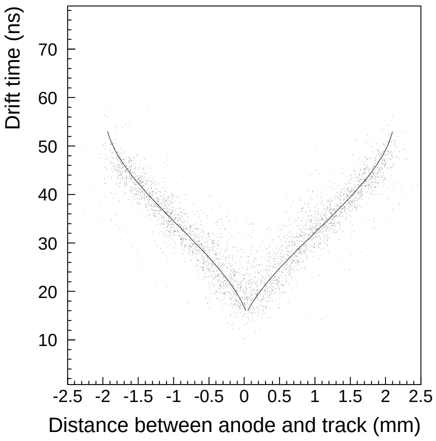

Fig. 3. A typical R-t dependence for one straw. The curves represent a fit using Eq. 1.

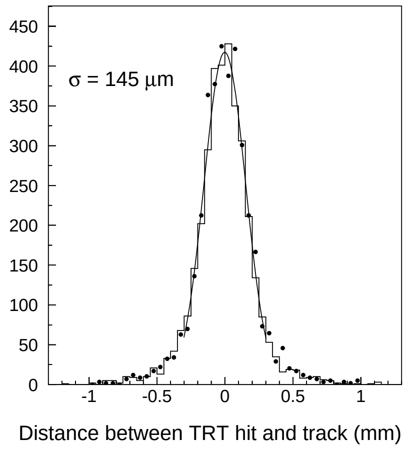

Fig. 4. Coordinate measurement accuracy for a single straw: distribution of the distance between the reconstructed hit and the extrapolated beam track position. The solid curve is a Gaussian fit to the data. The dots represent the Monte Carlo simulation.

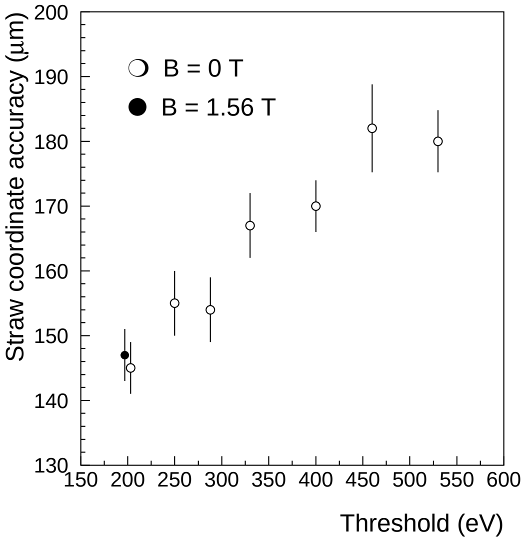

Fig. 5. The straw coordinate measurement accuracy obtained in the front TRT block as a function of the low-level electronics threshold and of the magnetic field. The error bars represent the accuracy variation from straw to straw.

pion beam.

The R-t dependencies of the straws were stable in time, but varied slightly from straw to straw due to differences in discriminator threshold, gas gain and possible anode wire eccentricity. The R-t dependence was measured explicitly for 8-10 straws in each TRT block (calibrated straws). For all the other straws, an average (so-called typical) R-t fit was used to reconstruct the hit position with respect to the anode. It was found that the difference in the coordinate measurement accuracy between the calibrated and the non-calibrated straws did not exceed $\sim$10%. Therefore, if a straw was not fully covered by the beam and thus could not be calibrated individually, the typical R-t dependence fit was used instead, with a loss of coordinate measurement accuracy of less than 10%.

5 Straw alignment

The R-t fit procedure, described above, provides a hit position with respect to the straw anode. To establish the hit position in an absolute coordinate system, a geometrical alignment should first be corrected out to obtain the coordinate of the anode wire. As a first approximation for the alignment procedure, the anode wire positions were determined by a mechanical survey during the TRT prototype installation in the beam area. The final alignment was done for each TRT straw individually using a large sample of beam tracks reconstructed by the silicon telescope and extrapolated to the TRT.

The alignment procedure was different for calibrated and non-calibrated straws. For the calibrated ones, the two-dimensional R-t plot and the corresponding fit were made with respect to the beam, *i.e.* in the Si-telescope coordinate system which was the reference system for the TRT measurements. In this case the alignment can be done by fitting the R-t dependence using the anode wire position as a free parameter. With a proper alignment, the intersection point of the two branches of the R-t fit (see Figure 3), should be found at R=0 mm. For the non-calibrated straws, no individual R-t fit was available and a typical one, which was aligned to R=0 mm by definition was therefore used. To obtain the best posible alignment, residual distributions similar to the one in Figure 4 were used. Such distributions were built for each of the non-calibrated straws crossed by the beam. The anode position was then obtained using the mean value of the Gaussian fit to the distribution.

The overall position of the TRT prototype was determined by setting to zero the average deviation of anode positions found by the alignment procedure from the expected positions based on the mechanical survey. The transverse beam size in front of the TRT was about 15 mm. As the distance between the anode wires in adjacent straws in one layer was 8.5 mm, two or three straws in each of the 80 TRT layers were covered by the beam. Hence, it was possible to compare the anode-to-anode distance inside one layer to the expected distance defined by the mechanical construction of the prototype. The difference between the measured and the expected anode-to-anode distance inside one TRT layer is shown in Figure 6. From this figure one can conclude that the average anode shift with respect to the expected position inside one layer did not exceed 60 μm. The value of 60 μm reflects the mechanical accuracy of the TRT prototype construction and the spread of possible anode wire eccentricities in the straws. It should therefore also represent the alignment accuracy for those straws, which were not covered by the beam and could not be aligned directly.

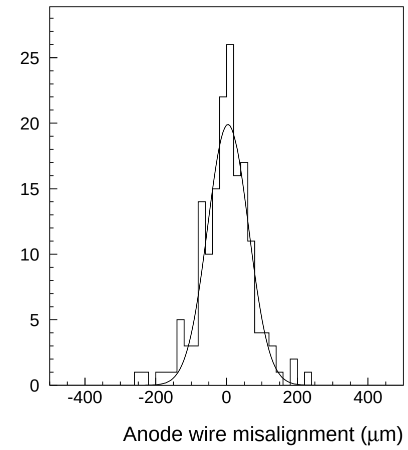

Fig. 6. The difference between the measured and the expected anode-to-anode distance inside one TRT layer obtained by the alignment procedure. The solid curve is a Gaussian fit to the data.

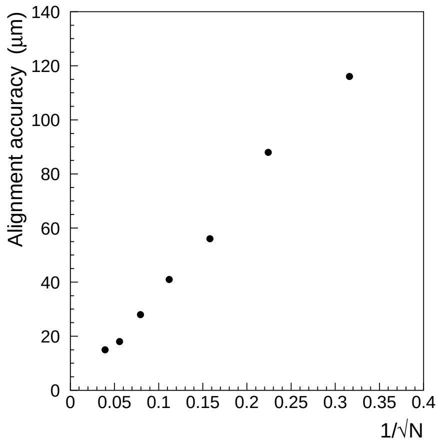

Fig. 7. Accuracy of the anode wire alignment as a function of $\sqrt{N}$, where N is the number of beam tracks used for alignment.

For the track reconstruction, the anode wire position has to be known with a precision much better than the coordinate accuracy of the drift-time measurement. The alignment precision depends not only on the intrinsic straw coordinate measurement accuracy, but also on the number of beam particles used for the alignment. The latter contribution can be estimated by measuring the anode wire position in the same straw several times using N particles in each measurement. The variation from measurement to measurement is an estimation of the alignment accuracy for a given value of N. Figure 7 shows the accuracy of the anode wire alignment as a function of the number of beam particles crossing the straw. For 100 tracks the alignment uncertainty is only about 30 μm. Note that one day of data-taking at the LHC initial low luminosity of 10^{33} cm^{-2}s^{-1} should be sufficient to collect almost 1000 muons per straw with $p_{\mathrm{T}} > 6$ GeV [1].

6 Hit registration efficiency

Two different hit registration efficiencies for the TRT straws can be defined. The first one or raw hit efficiency, was defined as the probability for obtaining a low-level threshold hit, if a beam particle crossed the straw. The second one or tracking hit efficiency, was defined as the probability that the hit belong to the reconstructed TRT track. This efficiency depends of course on the track reconstruction algorithm and is defined as the probability the hit lie inside a road of ± 400 μm around the reconstructed TRT track (see next section). The dependencies of both efficiencies on the low-level threshold are shown in Figure 8. At the nominal 200 eV threshold the raw hit efficiency is about 95% and the tracking hit efficiency is about 86%. One should take into account that the 5% raw hit inefficiency contains not only the intrinsic straw inefficiency, but also uncertainties in the beam track extrapolation inside the straw and residual geometrical misalignment.

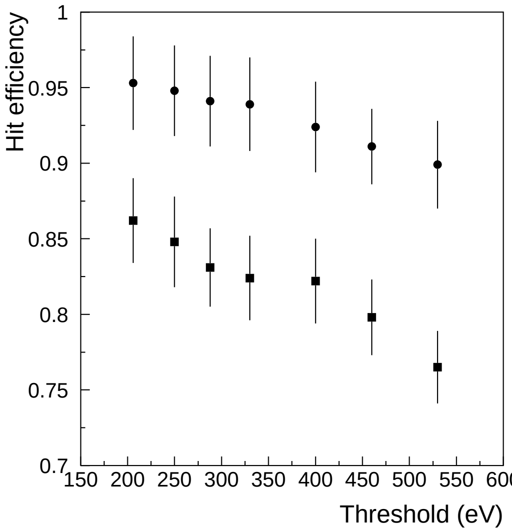

Fig. 8. Hit registration efficiency of TRT straws as a function of the low-level electronics threshold. The upper set of points corresponds to the overall probability to observe a hit in the straw (raw hit efficiency), and the lower set of points to the probability for the hit to belong to the reconstructed TRT track (tracking hit efficiency). The error bars represent the efficiency variation from straw to straw.

The straw noise probability was defined as the probability to obtain a low-level threshold hit in a straw when there was no beam particle crossing this straw. The reason for such noise signals can be particle interactions in upstream material or inside the TRT, high energy δ-electrons from a track passing close to the straw, but not crossing it, and noise or pickup in the electronics channel. The mean noise probability at 200 eV threshold was found to be 3.5%. A few straws with noise probability higher than 35% were excluded from the analysis.

7 Tracking with magnetic field off

A typical event from the run without magnetic field is displayed in Figure 9. Schematic views of the silicon detectors and of the TRT prototype in two different scales are shown.

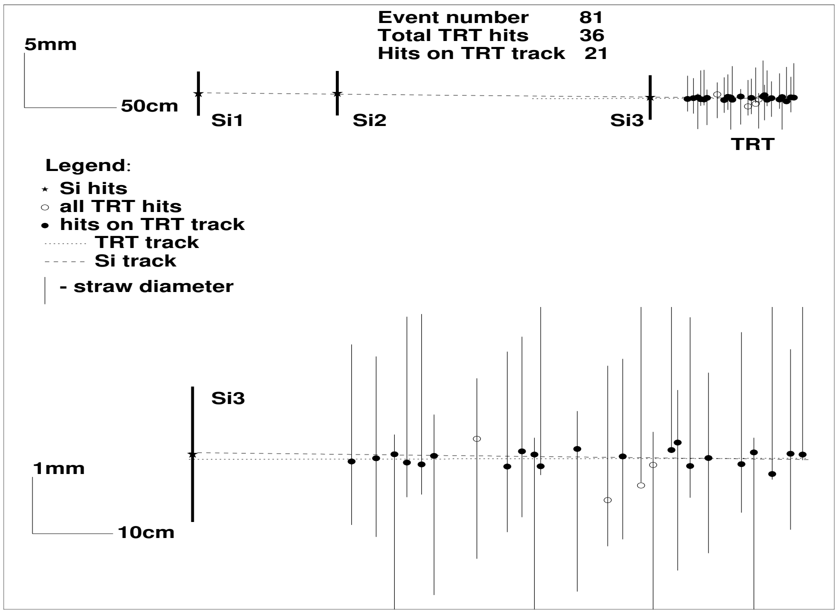

Fig. 9. Display of an event with magnetic field off. The TRT straws are drawn as vertical bars with a size corresponding to the straw diameter of 4 mm. Reconstructed hit positions inside the straws are shown as small circles. Two reconstructed tracks are drawn as dashed and dotted straight lines: they correspond respectively to the silicon telescope track and the TRT track.

The tracking procedure for the TRT prototype was iterative. In a first step, only information about the presence of a hit above the 200 eV threshold was used. The hit coordinate was assumed to be equal to the anode wire position. The TRT track was defined as a straight-line fit to these hit positions. In a second step, a road with width of $\pm\Delta$ around the TRT track was introduced. Only hits inside this road were taken into account. On the basis of the measured drift time, new hit coordinates were calculated from the R-t relation. To resolve the left-right ambiguity of the R-t relation, when both solutions were inside the road, the hit nearest to the TRT track was chosen. The coordinates of all the selected hits were then fitted to a straight line. This procedure was repeated several times by decreasing the width of the road step-by-step down to Δ=400 μm. Such a value was found to be optimal for the overall tracking accuracy, since for a final road width larger than 400 μm contamination from δ-electrons and from electronics noise and pickup degrade the accuracy of the track fit. For smaller final road widths, the number of hits belonging to the track decreases rapidly, which thereby reduces the track reconstruction accuracy. The distribution of the number of hits belonging to the reconstructed

TRT track after the final iteration is shown in Figure 10. The avarage number of hits is about 25.

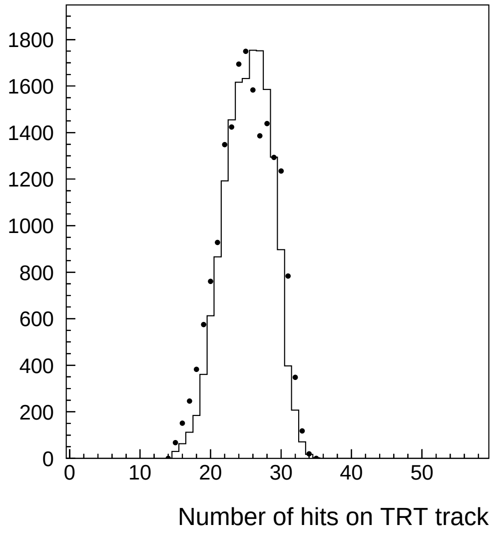

Fig. 10. The number of hits belonging to the reconstructed TRT track for 20 GeV pions from test-beam measurements (histogram) and from Monte Carlo simulation (dots).

The quality of the reconstructed TRT track can be specified in terms of angular and spatial accuracy. The angular accuracy is the r.m.s deviation of the track polar angle from the beam track. The spatial accuracy is defined as the r.m.s. distance between the reconstructed TRT track and the beam track at the centre of the sector prototype.

For more detailed studies of the TRT intrinsic spatial and angular accuracies, contributions arising from the beam track extrapolation and from multiple scattering in the material outside the TRT prototype should be eliminated. This was achieved by using the so-called odd-even technique. Each track in the TRT was reconstructed twice: first by using only odd-numbered hits in the current event, and then by using only even-numbered hits. The tracks thus obtained can be considered as independent measurements of the same original track, but with half the number of hits. If the angular difference between these two TRT tracks is found to be σ_0, then the intrinsic angular TRT accuracy σ_{TRT} can be retrieved from the relation $\sigma_0 = \sigma_{TRT} \cdot \sqrt{2} \cdot \sqrt{2}$. Here, one factor of $\sqrt{2}$ arises from the subtraction of the odd-numbered-hit track angle from the even-numbered-hit track angle in the σ_0 determination. The other factor of $\sqrt{2}$ is due to the fact that the tracks with "odd" and "even" hits have only half of the hits compared to the complete TRT track (the overall track accuracy is inversely proportional to the square root of the number of measurements). The same technique was applied to calculate the spatial TRT accuracy: the position difference between odd- and even-hit tracks in the middle of the TRT was calculated and divided by a factor of two.

The angular and spatial track accuracies, obtained as described above, are shown in Figures 11 and 12 for a 20 GeV pion beam. These plots display an average angular track accuracy of 0.18 mrad and spatial track accuracy of 40 μm for the sector prototype in the absence of a magnetic field.

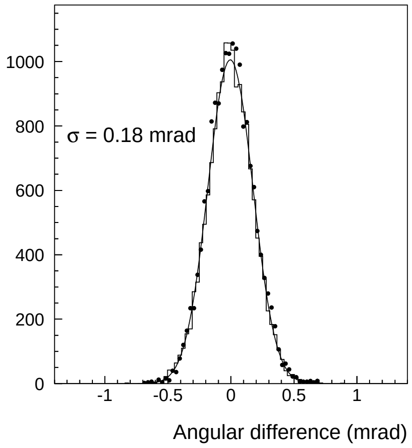

Fig. 11. Angular TRT track accuracy: difference between the angle of odd- and even-hit TRT tracks, divided by two (see text). The solid curve is a Gaussian fit to the experimental data (histogram) and the dots represent the Monte Carlo simulation.

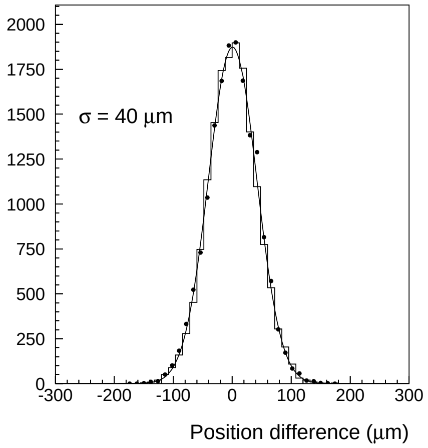

Fig. 12. Spatial TRT track accuracy: difference between the position of odd- and even-hit TRT tracks in the middle of the prototype, divided by two (see text). The solid curve is a Gaussian fit to the experimental data (histogram) and the dots represent the Monte Carlo simulation.

It should be noted that these angular and spatial accuracies still display some dependance on the beam-particle momentum, because of the contribution from multiple scattering inside the TRT material, which is not excluded by the odd-even procedure.

8 Tracking with magnetic field on

To examine the TRT tracking performance in the presence of a magnetic field, dedicated studies were performed in a magnetic field of 1.56 T. The setup is shown schematically in Figure 1. The magnetic field was oriented vertically, almost parallel to the straws. The first two Si detectors, Si1 and Si2, were placed outside the magnetic field and the third one, Si3, was placed inside, as close as possible to the sector prototype.

An event with the magnetic field on is displayed in Figure 13. The global reconstracted track was obtained as the result of a reconstruction procedure, where all three Si detectors and the TRT were involved in the fitting. For the track reconstruction the xKalman package [13] was adapted to the test-beam geometry. The xKalman program is based on the Kalman filter tracking algorithm [14]. It includes multiple scattering and bremsstrahlung effects and takes into account the non-uniformity of the magnetic field along the track.

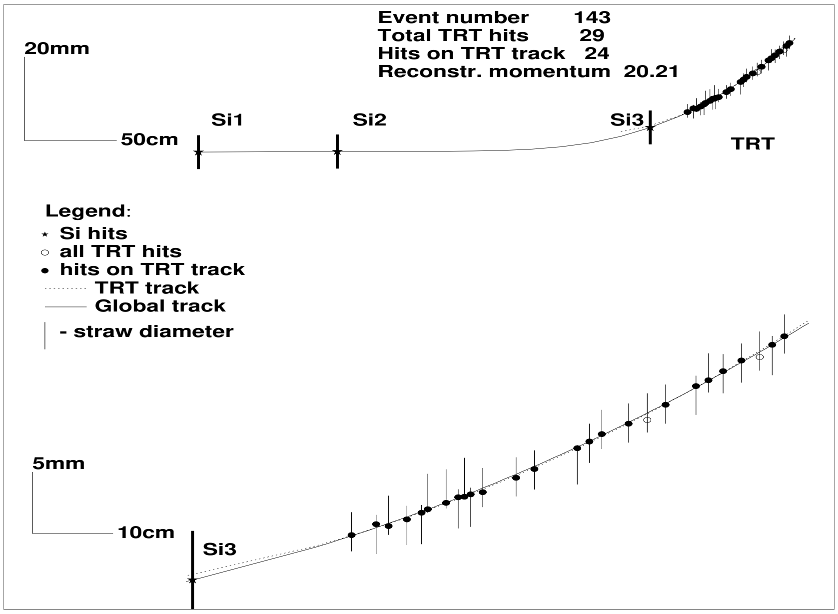

Fig. 13. Display of an event with the magnetic field on. The notations are the same as in Figure 9, except that the global track is shown as a solid line.

After the global track fitting, the straw performance was estimated in the same way as in the case without magnetic field: straw coordinate measurement accuracy, hit registration efficiency *etc.* The drift time of ionisation electrons in the straw gas was about 10% longer than without a magnetic field, so a re-fitting of the R-t dependences was performed. It was found that there is no significant difference in the single straw coordinate measurement accuracy whether the magnetic field is on or off (see Figure 5). The spatial track accuracy defined by the odd-even technique, as described above, was 44 μm, to be compared to 40 μm in the case without magnetic field.

The reconstructed momentum distributions for 20 GeV pions and electrons are shown in Figures 14 and 15 respectively. These figures show that the Gaussian part of the measured momentum is almost the same for electrons and pions, whereas the electrons display large non-Gaussian tails due to bremsstrahlung in the upstream material. One should also take into account that the intrinsic spread of the beam momentum is about 0.32% for the 20 GeV beam (and increases to about 0.62% for the 100 GeV beam) and therefore contributes significantly to the resolutions shown in Figures 14 and 15.

The momentum resolution dependence on the beam energy is shown in Fig-

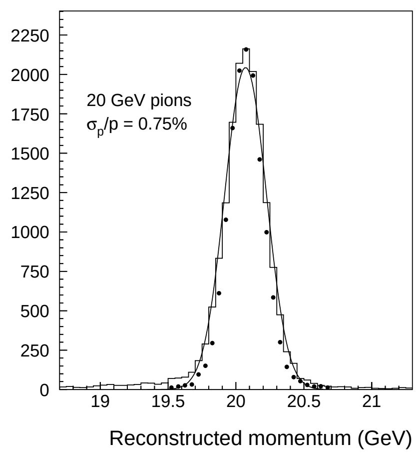

Fig. 14. Reconstructed momentum using the TRT and the three Si detectors for 20 GeV pions. (histogram). The solid curve is a Gaussian fit to the experimental data. The dots represent the Monte Carlo simulation.

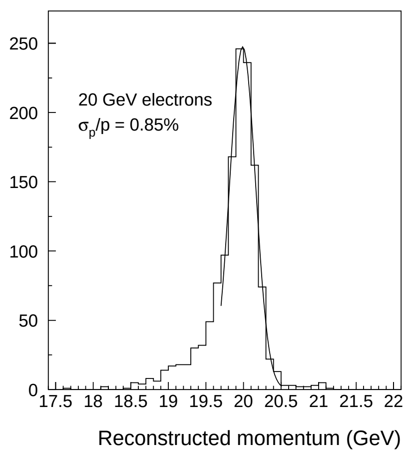

Fig. 15. Reconstructed momentum using the TRT and the three Si detectors for 20 GeV electrons (histogram). The solid curve is a Gaussian fit to the experimental data.

ure 16 for pions. The intrinsic beam momentum spread was subtracted in this case. The reconstruction results obtained without using hits from the third Si detector, placed inside the magnetic field, illustrate in a qualitative way the stand-alone performance of the TRT for momentum measurements with a beam constraint.

The momentum resolution dependence on the beam energy, obtained by using the TRT and either three or two Si detectors, displays the expected linear behaviour for beam energies above 40 GeV, with slopes of $2.3{\cdot}10^{-4}$/GeV and $3.8{\cdot}10^{-4}$/GeV for the 3Si's+TRT and 2Si's+TRT options respectively. For lower energies the momentum resolution is limited to 0.8% and 1.4% correspondingly, due to multiple scattering effects. When three Si detectors were used without the TRT, multiple scattering effects dominate over the intrinsic Si-detector coordinate measurement accuracy for the whole investigated beam energy region. Therefore the momentum resolution is almost independent of the beam particle momentum.

9 Conclusions

A sector prototype of the Transition Radiation Tracker (TRT) for the ATLAS experiment at LHC was built and tested with a series of measurements. The drift-time measurements, the alignment technique, the hit registration efficiency, and the track and momentum accuracies were studied. It is shown

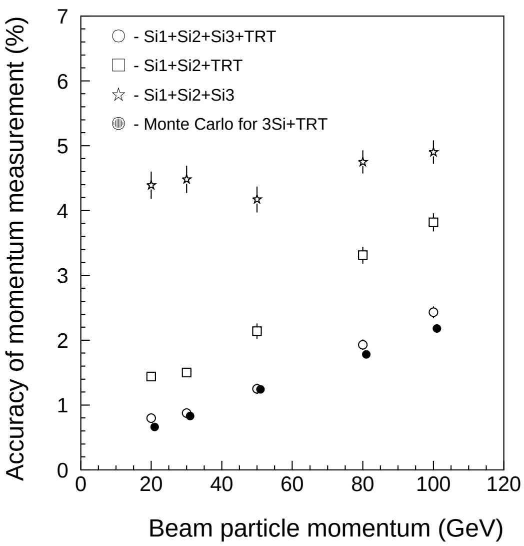

Fig. 16. Momentum resolution as a function of the charged pion momentum for different combinations of TRT and Si detectors in the test-beam.

that the single straw coordinate measurement accuracy is about 150 μm. An alignment accuracy of $\sim$30 μm can be achieved with 100 probe beam particles per straw. The hit efficiency is expected to be at least 95% at the nominal 200 eV threshold.

The accuracy achieved for the momentum measurement with the TRT prototype and the Si detectors varied from 0.8% to 2.4% for 20 GeV to 100 GeV pions in a 1.56 T magnetic field. Detailed Monte Carlo simulations described adequately the measured single straw and overall TRT tracking performance.

The above results give confidence in the reliability of the expected TRT performance in the ATLAS Inner Detector at the LHC.

10 Acknowledgements

We are very grateful to P. Norton, D.H. Saxon and D.J. White for their contributions to the read-out electronics used in this prototype test. We also thank K. Bussman, A. Konstantinov and G. Di Tore for their participation in the preparation of mechanics and electronics for the tests. The research described in this paper was partly supported by the International Science Foundation (grant NM5J000), the Polish State Committee for Scientific Research, the Swedish Natural Science Research Council and the Swedish Council for Planning and Coordination of Research.

References

[1] ATLAS Inner Detector Technical Design Report, CERN/LHCC/97-16, CERN/LHCC/97-17, 1997.

[2] T. Akesson *et al.*, *Nucl. Instrum. Meth.* **A 412** (1998) 200.

[3] M. Millmore, RAL internal note, RAL-118, 1992.

[4] D. White, RAL internal note, RAL-161, 1994.

[5] J. Dowdell, RAL internal note, RAL-117, 1992.

[6] H. Carling and M. Thulesius, Technical Specification of the RD6 Drift Time Measuring ReadOut Chip, Revision 3, Lund University internal report, LUNFD6(NFFL-7097), 1995.

[7] T. Akesson *et al.*, *Nucl. Instrum. Meth.* **A 367** (1995) 143.

[8] T. Akesson *et al.*, *Nucl. Instrum. Meth.* **A 449** (2000) 446.

[9] CN division Application Software group, GEANT detector description and simulation tool, CERN Program Library Long Writeup W5013, 1993

[10] A. Artamonov *et al.*, DICE-95, ATLAS internal note, ATLAS-SOFT/95-14, CERN, 1995.

[11] U. Egede and M. Stavrianakou, A modular simulation of prototypes in the H8 test-beam, ATLAS Internal Note ATL-INDET-97-173, 1997.

[12] V.M. Grishin, V.K. Ermilova and S.K. Kotelnikov, *Nucl. Instrum. Meth.* **A 307** (1991) 273.

[13] I. Gavrilenko, Description of Global Pattern Recognition Program (xKalman), ATLAS Internal Note ATL-INDET-97-165, 1997.

[14] R. Fruhwirth, *Nucl. Instrum. Meth.* **A 262** (1987) 444.